

Etomidate-induced myoclonus correlates with the dysfunction of astrocytes and glutamate transporters in the neocortex of Sprague-Dawley rats

Y. FENG^{1,2}, J. LIU^{1,2}, W.-S. ZHANG^{1,2}

¹Department of Anesthesiology, Laboratory of Anesthesia and Critical Care Medicine, Translational Neuroscience Center, ²National-Local Joint Engineering Research Center of Translational Medicine of Anesthesiology, West China Hospital, Sichuan University, Chengdu, China

Abstract. – OBJECTIVE: Etomidate-induced myoclonus is common in clinical anesthesia. Propofol and lidocaine, as other sedative hypnotic and anticonvulsant drugs, rarely induce myoclonus. The mechanism of the myoclonus remains unclear.

MATERIALS AND METHODS: Eighty-four adult male Sprague-Dawley (SD) rats anesthetized intravenously with etomidate, propofol, or lidocaine plus etomidate were observed of the behavioral changes at 0, 1, 2, 3, 4 and 5 min after anesthesia. Five minutes later, glutamate levels were measured in the cerebrospinal fluid (CSF), neocortex and hippocampus. The mRNAs and proteins expression of EAAT1, EAAT2, and GFAP in the neocortex and hippocampus were analyzed by quantitative real-time polymerase chain reaction (qRT-PCR), Western blot and immunofluorescence staining.

RESULTS: Etomidate increased the mean behavioral scores at different time points and the neocortical glutamate level compared with the propofol ($p=0.0283$) and the lidocaine plus etomidate group ($p=0.0035$); The correlation analysis revealed a strong correlation between the mean behavioral score and the neocortical glutamate content (Spearman's $r=0.6638$, $p=0.0027$). No significant difference was found in the EAAT1, EAAT2, or GFAP mRNAs in the neocortex and hippocampus among three groups; etomidate decreased EAAT1 ($p=0.0416$ and $p=0.0127$) and EAAT2 ($p=0.0363$ and $p=0.0109$) proteins but increased the GFAP ($p=0.0145$ and $p=0.0149$) protein in the neocortex compared to the propofol and lidocaine plus etomidate group. Furthermore, etomidate activated GFAP-positive cells in the neocortex, but conversely inhibited proteins of EAATs in motor cortex.

CONCLUSIONS: Etomidate-induced myoclonus is associated with neocortical glutamate accumulation. Suppression of the astrogliosis in neocortex and promoting extracellular glutamate uptake by regulating glutamate transporters (EAATs) in the motor cortex may be the therapeutic target for prevention of etomidate-induced myoclonus.

Etomidate, Myoclonus, Glutamate transporter, Astrocytes.

Key Words:

Etomidate, Myoclonus, Glutamate transporter, Astrocytes.

Abbreviations

GLT: glutamate transporters; EAAT1: Excitatory amino acid transporter 1; EAAT2: Excitatory amino acid transporter 2; GFAP: glial fibrillary acidic protein; RT-PCR: real-time polymerase chain reaction; SD: Sprague-Dawley; CSF: Cerebrospinal fluid; LC-MS/MS: liquid chromatography coupled with tandem mass spectrometric; IS: Ion spray; BCA: bicinchoninic acid; PVDF: polyvinylidene difluoride; DAPI: 4',6-diamidino-2-phenylindole; PBS: phosphate buffered saline; RSA: retro splenic agranular; ANOVA: analysis of variance; HRP: horseradish peroxidase; GABA: γ -aminobutyric acid; PKA: protein kinase A; PKC: protein kinase C and PI3K: phosphatidylinositol-3-kinase.

Introduction

Etomidate, as a sedative hypnotic anesthetic, is widely used in clinical anesthesia. Etomidate-related myoclonus with a high incidence of 80%¹ is a sudden and brief involuntary twitching or jerking of a muscle or group of muscles that can last from seconds to minutes during anesthesia induction². The myoclonus can lead to serious complications, such as accidental

dislocation of intravenous tubes or monitoring devices, difficulty in airway management and increased potassium blood levels³. To our knowledge, propofol, as another sedative hypnotic drug, rarely induces myoclonus (1%)⁴, while both propofol and lidocaine can prevent the etomidate-induced myoclonus^{5,6}. Although some studies found that etomidate-induced myoclonus is a seizure-like activity⁷, the accurate mechanism remains unknown. R ath et al⁸ demonstrated that etomidate increased the glutamate concentration by inhibiting glutamate uptake through the blockade of GLTs (glutamate transporters) in rat cultured glial cells. Extracellular glutamate levels play a crucial role in modulating the extent of neuronal excitability, and an imbalance of glutamate release and uptake may be associated with seizures⁹. Excitatory amino acid transporter 1 (EAAT1) and excitatory amino acid transporter 2 (EAAT2) are predominantly expressed in astroglial cells and are responsible for approximately 90% and 5-10% of glutamate uptake, respectively^{10,11}. However, the effect of etomidate on the function of EAATs following myoclonus has not been verified.

Astrocytes are the largest and most abundant glial cells, which act as a critical component of tripartite synapses and participate in ionic homeostasis, energy metabolism and the modulation of synaptic transmission¹². Intermediate filament glial fibrillary acidic protein (GFAP) is often measured to observe astrocytic shape and function, and striking changes in reactive astrocytes may result in increased neuronal excitability¹³. GFAP may have direct or indirect epileptogenic functions on astrocytes¹⁴⁻¹⁶. The effects on the function of astrocytes during anesthesia are rarely reported.

Except for that, etomidate-induced a seizure-like activity in the neocortex, as well as in the hippocampus in brain slices¹⁷. However, the associated location of etomidate-induced myoclonus remains unknown. To explore the mechanism of etomidate-induced myoclonus and the effect of etomidate on the functions of EAATs and astrocyte following myoclonus, we investigated the alterations of glutamate in the cerebrospinal fluid, neocortex and hippocampus, GFAP and EAATs in the neocortex and hippocampus through real-time polymerase chain reaction (RT-PCR), Western blot, and immunofluorescence analysis in a Sprague-Dawley (SD) rat model during anesthesia with etomidate, propofol, or lidocaine plus etomidate.

Materials and Methods

Animals

All experimental animal procedures were approved by the Animal Ethics Committee of West China Hospital, Sichuan University (Ethical Approval No. 20211423A) and conducted in strict accordance with the Guide for the Care and Use of Laboratory Animals published by the United States National Institutes of Health¹⁸. Adult male SD rats weighing 200-340 g (6-8 weeks old) were purchased from Dossy Biological Technology Co., Ltd. (Chengdu, China). All rats were housed at 25 ± 1°C with 60% humidity in the Animal Experimental Centre of Sichuan University (Chengdu, China) on a 12-hour light/dark cycle (lights on at 7:00 a.m.) and provided ad libitum access to water and food. The rats were habituated to the experimental environment 1 week before testing. The rats were numbered, randomly assigned to experimental groups using a random number table and tested in sequential order.

Anesthesia and Quantification of the Behavioral Activity in Rats

Adult male SD rats in the three groups received etomidate (1.5 mg kg⁻¹, YT200712, Nhwa Pharmaceutical Corporation, Xuzhou, China), propofol (11.824 mg kg⁻¹, X19055B, AstraZeneca UK, London, UK) or lidocaine (4 mg kg⁻¹, 2105J05, Zhaohui Pharmaceutical Corporation, Shanghai) plus etomidate (1.5 mg kg⁻¹) through the caudal vein. Then, the rats were placed in isolated transparent cages and observed at 0, 1, 2, 3, 4 and 5 min to monitor behavioral changes after anesthesia. The behavioral activity in rats was scored using the method described in previous studies¹⁸⁻²⁰, as follows: stage 0, no response; stage 1, ear and facial twitching; stage 2: myoclonic jerks without rearing; stage 3: myoclonic jerks and rearing; stage 4: turning over onto the side and tonic-clonic seizures; and stage 5: turning over onto the back and generalized tonic-clonic seizures.

Cerebrospinal Fluid (CSF) and Tissue Sample Collection

After intravenous anesthesia with etomidate, propofol, or lidocaine plus etomidate for 5 min, 84 rats in the three groups were sacrificed by decapitation. The cerebrospinal fluid of 6 rats in each group was collected for glutamate measurement, and the neocortical and hippocampal tissues of 6 rats in each group were collected in frozen pipes and stored at -80°C for glutamate

measurement and Western blotting. The neocortical and hippocampal tissues of other 6 rats in each group were collected in frozen pipes with RNA preservation solution for quantitative real-time polymerase chain reaction (qRT-PCR). The whole brains of the remaining 4 rats in each group were collected for tissue slicing for immunofluorescence tests.

Measurement of Glutamate

Adult male SD rats were fixed in a stereotactic frame after anesthesia with etomidate, propofol, or lidocaine plus etomidate. Five minutes later, 100-150 μ l of CSF²¹ and neocortical and hippocampal tissues²² were extracted and the two latter were homogenized using a high-throughput tissue grinder (SCIENTZ-48) in ice-cold 0.9% normal saline at a mass-to-volume ratio of 1:10 and then centrifuged to precipitate the proteins (Allegra™ 64R centrifuge, USA; 10,000 \times g, 10 min, 4°C). The supernatant was collected for further analyses. The liquid chromatography coupled with tandem mass spectrometric (LC-MS/MS) system consisted of an Agilent 6460 triple quadrupole mass spectrometer equipped with an electrospray ionization source (Agilent Technologies, Santa Clara, CA, USA), and the ion spray (IS) method was used to determine the glutamate content. The following parameters were used: column temperature of 35°C, dry gas flow rate of 5.0 L/min, dry gas temperature of 350°C, sheath gas flow rate of 11.0 L/min, sheath gas heater temperature of 350°C, nebulizer pressure of 45 psi, capillary voltage of 3,500 V, and auxiliary voltage of 500 V. The data were analyzed using Mass Hunter software (Build 4.0.479.0, Agilent Technologies).

Quantitative Real-Time Polymerase Chain Reaction Analysis

Total RNA in the neocortex and hippocampus of each rat was extracted with TRIzol reagent

(TaKaRa, Otsu, Shiga, Japan, #9109) at a low temperature on a clean bench (SW-CJ-1D, China). The RNA from each sample was used to synthesize cDNA using a High-Capacity cDNA Reverse Transcription Kit (Toyobo, Tokyo, Japan, #FSQ-201) with the Automatic Medical PCR Analysis System (SCILOGEX, Shanghai, China). The sequences for the primers are shown in Table I.

The total RNA concentration was determined using an ultramicro spectrophotometer (Scandrop 100, China). qRT-PCR was performed on an Automatic Medical PCR Analysis System with SYBR® Green Real-time PCR Master Mix in a final volume of 20 μ l, with the following thermal cycling conditions: 95°C for 2 min, followed by 40 cycles of 95°C for 10 s, 58°C for 30 s, and 95°C for 15 s. A GAPDH positive control without template was included for each amplification. The above real-time fluorescence quantification was repeated three times to obtain three Ct values, and the average Ct value was calculated. The data module was derived by the PCR software system, and the expression of EAAT1, EAAT2, and GFAP mRNA was quantitatively analyzed according to the $RQ=2^{-\Delta\Delta CT}$ method.

Western Blot Analysis

Protein levels of EAAT1, EAAT2 and GFAP were measured by Western blotting. Briefly, proteins were extracted from neocortical and hippocampal tissues using radioimmunoprecipitation assay buffer (#P0013B, Beyotime, Shanghai, China) containing a protease inhibitor cocktail (Roche Diagnostics GmbH, Mannheim, Germany), and total protein concentrations were measured by using a bicinchoninic acid (BCA) protein concentration determination kit (#P0010, Beyotime, Shanghai, China). Proteins were separated on 8% SDS-PAGE gels and then transferred onto polyvinylidene difluoride (PVDF) membranes (Millipore, Billerica, MA, USA; #IS-

Table I. Primer sequences used for the PCR analysis.

Gene	Sequences	
EAAT1	Forward	5'-TCAGAACATCACCAAGGAGGA-3'
	Reverse	5'-TACGGTCGGAGGGCAA-3'
EAAT2	Forward	5'-AGCCAAAGCACCGAAACC-3'
	Reverse	5'-AAGCAGCCCGCCACATA-3'
GFAP	Forward	5'-TGGAGATACTTGGACAATGGA-3'
	Reverse	5'-AGACCTTCACACTGAGACGC-3'
GAPDH	Forward	5'-GGTGAAGGTCTGGTGTGAACG-3'
	Reverse	5'-CTCGCTCCTGGAAGATGGTG-3'

EQ00010). After blocking with 5% non-fat dry milk solution for 2 hours at room temperature, the membranes were incubated with primary antibodies at 4°C overnight (EAAT1, Cell Signaling Technology, Danvers, MA, USA; #5684, 1:1,000 dilution; EAAT2, Proteintech, #22515-1-AP, 1:1,000 dilution; GFAP, Cell Signaling Technology, #3670, 1:1,000 dilution). After washing with PBST three times for 5 min each time, the membranes were incubated with the appropriate horseradish peroxidase (HRP)-conjugated goat anti-rabbit secondary antibody (1:5,000, #ZB2301 ZSGB-BIO, China) for 2 hours at room temperature, developed with Clarity™ Western ECL Substrate (#170-5060, Bio-Rad, Hercules, CA, USA) or an Omni-ECL™ Femto Light Chemiluminescence Kit (#SQ201, Yamei, China), and immediately imaged on an Amersham Imager 600 instrument (GE, USA). The bolts were stripped and washed with the stripping buffer (Thermo Scientific, Waltham, MA, USA #21059), then the membranes were incubated with the primary antibodies at 4°C overnight (rabbit anti-alpha tubulin, Proteintech, China, #11224-1-AP, 1:4,000) and the appropriate HRP-conjugated goat anti-rabbit secondary antibody. The intensity of the protein bands was normalized to alpha tubulin.

Immunofluorescence Staining

Adult male SD rats were anesthetized with etomidate, propofol, or lidocaine plus etomidate; 5 min later, the rats were decapitated, and the brains were dissected and placed in 4% paraformaldehyde for 24 h. Fixed brains were then cryoprotected in a high sucrose solution until the tissues sank to the bottom²³. The coronal sections were cut into 6 µm sections using a low temperature thermostat (Leica, Germany). For immunofluorescence staining, sections were first washed three times with PBS and then blocked with 10% normal goat serum for 30 min at 37°C. Then, the sections were incubated overnight with the following primary antibodies at 4°C: rabbit anti-EAAT1 (Cell Signaling Technology, #5684, 1:1,000 dilution); rabbit anti-EAAT2 (Proteintech, #22515-1-AP, 1:1,000 dilution); mouse anti-GFAP (Cell Signaling Technology, #3670, 1:1,000 dilution). The next day, the sections were rinsed three times with PBS and incubated with the following corresponding secondary antibodies for 2 h at 37°C: Cy3-conjugated goat anti-mouse IgG (1:100, Servicebio, Cat. No. GB21301); Fluor 488-conjugated goat anti-rabbit IgG (1:100, Servicebio, Cat. No. GB22303). Then, sections

were washed three times in phosphate buffered saline (PBS) and incubated with 4',6-diamidino-2-phenylindole (DAPI) (Beyotime) for nuclear staining at 37°C for 10 min. Negative control sections were incubated with PBS, and micrographs were analyzed using a fluorescence confocal microscope (Olympus, Japan). To determine the immunoreactivity of EAAT1, EAAT2, and GFAP in the neocortex, retro splenial agranular (RSA) cortex, motor cortex, and somatosensory cortex, five slices from each rat were arbitrarily selected (n=4 rats per group and 5 images per animal).

Statistical Analysis

Statistical analyses were performed using Prism 9.0.0 software (GraphPad Software, San Diego, CA, USA) and SPSS software, version 19.0 (IBM Corp., Armonk, NY, USA). Parametric data were reported as the means and standard deviations, and nonparametric data were reported as percentiles. The number of animals used was reported as the “n”. A normal distribution was confirmed using the Shapiro-Wilk test. The group size was determined using the method described in previous studies²⁴. The mean behavioral score at different times among the three groups were determined by two-way multiple comparisons analysis of variance (ANOVA), and the measurements of glutamate in neocortex and hippocampus were determined by one-way multiple comparisons ANOVA. Spearman correlation analysis was used to identify the relationship between the mean behavioral score and the glutamate content in the neocortex or hippocampus. The expression of EAAT1, EAAT2, and GFAP mRNAs and proteins in the neocortex and hippocampus, the mean grey value of the neocortex, and the ratio of GFAP-positive cells to total cells in the neocortex or hippocampus were analyzed by one-way multiple comparisons ANOVA or two-tailed *t*-test in groups for normally distributed data and the Kruskal-Wallis' test or two-tailed Mann-Whitney U test for non-normally distributed data. Statistical significance was set at $p < 0.05$.

Results

Etomidate-Induced Myoclonus and Increased the Glutamate Level in the Neocortex

The behavioral scores were recorded at different time points in the etomidate, propofol, and lidocaine plus etomidate groups (Figure 1A), and

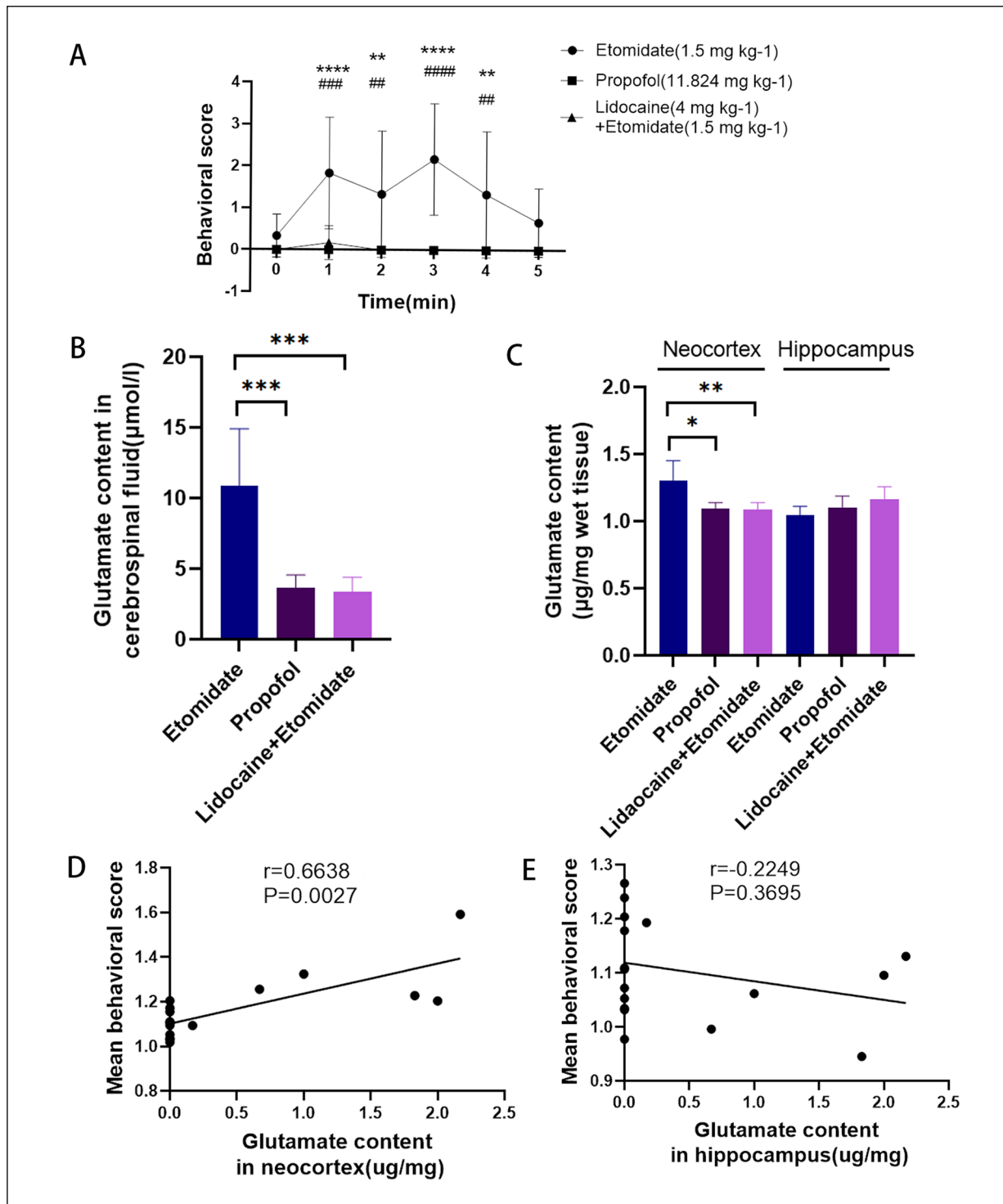


Figure 1. Quantifications of etomidate-induced myoclonus and glutamate measurement. The trend of behavioral scores at different time points in the etomidate, propofol, lidocaine plus etomidate group (A), as determined by two-way multiple comparisons ANOVA. Glutamate content in CSF (B), neocortex and hippocampus (C) in the etomidate, propofol, and lidocaine plus etomidate group (n=6 rats in each group), and one-way multiple comparisons ANOVA was applied to analyze difference. Spearman correlation analysis of the relationship between the mean behavioral score and glutamate content in neocortex ($r=0.6638$, $p=0.0027$, D) and hippocampus ($r=0.135$, $p=0.4768$, E). *: $p<0.05$; **: $p<0.01$; ***: $p<0.001$; ****: $p<0.0001$, compared to the propofol group; #: $p<0.05$; ##: $p<0.01$; ###: $p<0.001$; ####: $p<0.0001$, compared to the lidocaine plus etomidate the group. CSF: Cerebrospinal fluid; ANOVA: Analysis of variance.

etomidate increased the mean behavioral scores at 1 min (1.83 ± 1.33 vs. 0.00 ± 0.00 , $n=6$, $p < 0.0001$; 1.83 ± 1.33 vs. 0.17 ± 0.41 , $n=6$, $p=0.0003$), 2 min (1.33 ± 1.51 vs. 0.00 ± 0.00 , $n=6$, $p=0.0048$ for both), 3 min (2.17 ± 1.33 vs. 0.00 ± 0.00 , $n=6$, $p < 0.0001$ for both), and 4 min (1.33 ± 1.51 vs. 0.00 ± 0.00 , $n=6$, $p < 0.0048$ for both) and did not affect the mean behavioral scores at 0 min (0.33 ± 0.52 vs. 0.00 ± 0.00 , $n=6$, $p=0.6985$ for both) and 5 min (0.67 ± 0.82 vs. 0.00 ± 0.00 , $n=6$, $p=0.243$ for both) after administration compared to the propofol and lidocaine plus etomidate group, as determined by two-way multiple comparisons ANOVA. Etomidate increased the glutamate level in rats' CSF compared with the propofol (10.90 ± 4.01 vs. 3.64 ± 0.92 $\mu\text{mol/l}$, $n=6$; $p=0.0003$) and the lidocaine plus etomidate (10.90 ± 4.01 vs. 3.39 ± 1.03 $\mu\text{mol/l}$, $n=6$; $p=0.0002$) (Figure 1B). In the neocortex, etomidate increased the glutamate level compared with the propofol group (1.30 ± 0.15 vs. 1.09 ± 0.04 $\mu\text{g/mg}$, $n=6$; $p=0.0283$) and the lidocaine plus etomidate group (1.30 ± 0.15 vs. 1.08 ± 0.05 $\mu\text{g/mg}$, $n=6$; $p=0.0035$). In the hippocampus, etomidate did not affect the glutamate level (1.04 ± 0.07 vs. 1.10 ± 0.08 $\mu\text{g/mg}$, $n=6$, $p=0.4157$; 1.04 ± 0.07 vs. 1.16 ± 0.09 $\mu\text{g/mg}$, $n=6$, $p=0.0536$) compared to the propofol, and lidocaine plus etomidate group, as determined by one-way multiple comparisons ANOVA (Figure 1C). The correlation analysis revealed a strong correlation between the mean behavioral score in three groups and the neocortical glutamate content (Spearman's $r=0.6638$,

$p=0.0027$) (Figure 1D), but no relationship between the mean behavioral score and the hippocampal glutamate content was found (Spearman's $r=0.135$, $p=0.4768$) (Figure 1E).

Etomidate Did Not Affect the mRNA Expression of EAAT1, EAAT2, or GFAP in the Neocortex or Hippocampus

Etomidate did not affect the mRNA expression of EAAT1 in the neocortex (0.99 ± 0.15 vs. 0.91 ± 0.08 , $n=6$, $p=0.4453$; 0.99 ± 0.15 vs. 0.86 ± 0.12 , $n=6$, $p=0.1511$) or the hippocampus (0.93 ± 0.14 vs. 0.84 ± 0.17 , $n=6$, $p=0.6252$; 0.93 ± 0.14 vs. 0.78 ± 0.18 , $n=6$, $p=0.2737$) compared with the propofol group and lidocaine plus etomidate group (Figure 2A). Etomidate affected neither the mRNA expression of EAAT2 in the neocortex (1.09 ± 0.18 vs. 1.04 ± 0.07 , $n=6$, $p=0.7837$; 1.09 ± 0.18 vs. 0.99 ± 0.13 , $n=6$, $p=0.4030$) and the hippocampus (1.05 ± 0.10 vs. 0.91 ± 0.13 , $n=6$, $p=0.0803$), nor the mRNA levels of GFAP in the neocortex (1.01 ± 0.18 vs. 1.03 ± 0.22 , $n=6$, $p=0.9909$; 1.01 ± 0.18 vs. 0.88 ± 0.24 , $n=6$, $p=0.5452$) and the hippocampus (2.25 ± 0.85 vs. 2.29 ± 0.90 , $n=6$, $p=0.9964$; 2.25 ± 0.85 vs. 2.39 ± 0.76 , $n=6$, $p=0.9560$) compared to the propofol group and lidocaine plus etomidate group (Figure 2B), as determined by one-way multiple comparisons ANOVA. However, the mRNA expression of GFAP in the hippocampus was significantly higher than that in the neocortex in the etomidate ($p=0.0273$),

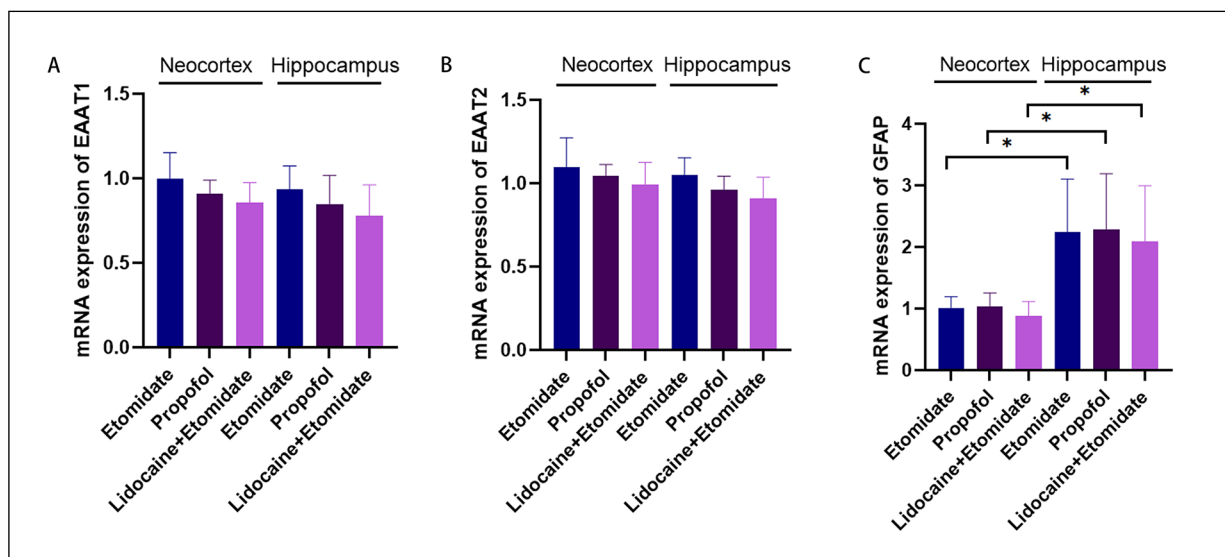


Figure 2. mRNA expression of EAAT1, EAAT2, GFAP in neocortex and hippocampus. Expression of EAAT1(A), EAAT2 (B), GFAP (C) mRNA in neocortex and hippocampus in the etomidate, propofol, and lidocaine plus etomidate group. One-way multiple comparisons ANOVA was applied to analyze difference. *: $p < 0.05$.

propofol ($p=0.0254$), and lidocaine plus etomidate ($p=0.0013$) group, as determined by paired t -test (Figure 2C).

Etomidate Decreased the Expression of EAAT1 and EAAT2 Proteins, but Conversely Increased the Expression of GFAP Protein in the Neocortex

In the neocortex, etomidate decreased not only the EAAT1 protein expression (0.81 ± 0.09 vs. 1.07 ± 0.18 , $n=6$, $p=0.0416$; 0.81 ± 0.09 vs. 1.13 ± 0.19 , $n=6$, $p=0.0127$) (Figure 3A and B), but also the EAAT2 protein expression (0.61 ± 0.29 vs. 1.11 ± 0.25 , $n=6$, $p=0.0363$; 0.61 ± 0.29 vs. 1.22 ± 0.38 , $n=6$, $p=0.0109$) (Figure 3C and D) compared to the propofol group and the lidocaine plus etomidate group. Conversely, etomidate increased GFAP protein expression compared to the propofol group (0.86 ± 0.15 vs. 0.59 ± 0.16 , $n=6$, $p=0.0145$) and the lidocaine plus etomidate group (0.86 ± 0.15 vs. 0.59 ± 0.12 , $n=6$, $p=0.0149$) (Figure 3E and F). In the hippocampus, etomidate did not affect EAAT1 protein expression compared to the propofol or lidocaine plus etomidate (1.16 ± 0.33 vs. 0.99 ± 0.19 , $n=6$, $p=0.4870$; 1.16 ± 0.33 vs. 1.11 ± 0.24 , $n=6$, $p=0.8019$) (Figure 3A and B). As for the EAAT2 protein, etomidate decreased the expression compared to the propofol (0.68 ± 0.26 vs. 1.04 ± 0.16 , $n=6$, $p=0.0245$), but no significant difference was found between the etomidate and the lidocaine plus etomidate group (0.68 ± 0.26 vs. 0.87 ± 0.21 , $n=6$, $p=0.2864$) (Figure 3C and D). Additionally, etomidate did not affect the GFAP protein expression (1.29 ± 0.21 vs. 1.37 ± 0.19 , $n=6$, $p=0.8649$; 1.29 ± 0.21 vs. 1.39 ± 0.27 , $n=6$, $p=0.7857$) (Figure 3E and F) compared to the propofol and lidocaine plus etomidate group, as determined by one-way multiple comparisons ANOVA. Furthermore, etomidate upregulated the expression of EAAT1 ($p=0.0326$) and GFAP ($p=0.0051$) in the hippocampus compared to that in the neocortex, and both propofol ($p=0.0003$) and lidocaine plus etomidate ($p=0.0010$) upregulated the expression of GFAP in the hippocampus compared to that in the neocortex, as determined by paired t -test and two-tailed Mann-Whitney U test. In addition, double immunofluorescence staining revealed that EAAT1 and EAAT2 were mainly expressed on astrocytes (Figure 3H and G).

Etomidate Activated Astrocytes in the Neocortex Not Hippocampus

To investigate whether changes in the astrocytic response are involved in the pathogenesis of etomidate-induced myoclonus, a semiquantita-

tive immunofluorescence analysis of GFAP was performed (Figure 4 and Figure 5). In the neocortex, the ratio of GFAP-positive cells to total cells in the etomidate group was significantly increased compared to the propofol (30.80 ± 2.53 vs. $15.70\pm 2.45\%$, $n=4$, $p=0.0002$) and lidocaine plus etomidate group (30.80 ± 2.53 vs. $11.63\pm 3.98\%$, $n=4$, $p<0.0001$) (Figure 4D). In terms of morphology, astrocytes in the etomidate group seemed to be hypertrophic compared to those in the other two groups (Figure 4A-C and A'-C'); In the hippocampus, etomidate did not affect the ratio of GFAP-positive cells to total cells compared to the propofol and lidocaine plus etomidate group (44.53 ± 3.99 vs. $42.83\pm 5.75\%$, $n=4$, $p=0.8704$; 44.53 ± 3.99 vs. $44.90\pm 4.35\%$, $n=4$, $p=0.9932$) (Figure 5D), as determined by one-way multiple comparisons ANOVA. The cells in three groups were similar in morphology (Figure 5A-C and A'-C').

Etomidate Inhibited the Expression of EAAT1 and EAAT2 Proteins in the Motor Cortex

To compare the expression of EAAT1 and EAAT2 in more specific regions of the neocortex (RSA cortex, motor cortex, and somatosensory cortex) and hippocampus, we used an immunofluorescence approach. As shown in Figure 6A-F and Figure 7A-F, etomidate inhibited the mean grey values of EAAT1 and EAAT2 in the motor cortex compared to propofol (42.80 ± 3.47 vs. 59.92 ± 4.35 , $n=4$; 36.93 ± 4.45 vs. 59.11 ± 5.63 , $n=4$, $p=0.0013$ for both) and lidocaine plus etomidate (42.80 ± 3.47 vs. 52.93 ± 5.59 , $n=4$, $p=0.0280$; 36.93 ± 4.45 vs. 46.09 ± 2.98 , $n=4$, $p=0.0490$). Etomidate did not affect the mean grey value of EAAT1 in the RSA cortex (43.58 ± 1.44 vs. 48.18 ± 16.49 , $n=4$, $p=0.8000$; 43.58 ± 1.44 vs. 51.26 ± 5.63 , $n=4$, $p=0.5517$), somatosensory cortex (46.39 ± 3.49 vs. 49.65 ± 14.45 , $n=4$, $p=0.8707$; 46.39 ± 3.49 vs. 56.22 ± 5.39 , $n=4$, $p=0.3258$), or hippocampus (33.11 ± 6.39 vs. 34.02 ± 13.74 , $n=4$, $p=0.9919$; 33.11 ± 6.39 vs. 33.10 ± 10.42 , $n=4$, $p>0.9999$) compared to the propofol and lidocaine plus etomidate group. Etomidate affect the mean grey value of EAAT2 neither in the RSA cortex (47.98 ± 8.66 vs. 56.28 ± 6.37 , $n=4$, $p=0.7179$; 47.98 ± 8.66 vs. 47.40 ± 5.07 , $n=4$, $p>0.9999$) nor in the hippocampus (32.78 ± 12.02 vs. 30.67 ± 10.63 , $n=4$, $p=0.9667$; 32.78 ± 12.02 vs. 31.81 ± 13.16 , $n=4$, $p=0.9928$) compared to the propofol and lidocaine plus etomidate group. Lidocaine plus etomidate (45.77 ± 2.55 vs. 40.54 ± 5.39 , $n=4$, $p=0.3546$) did

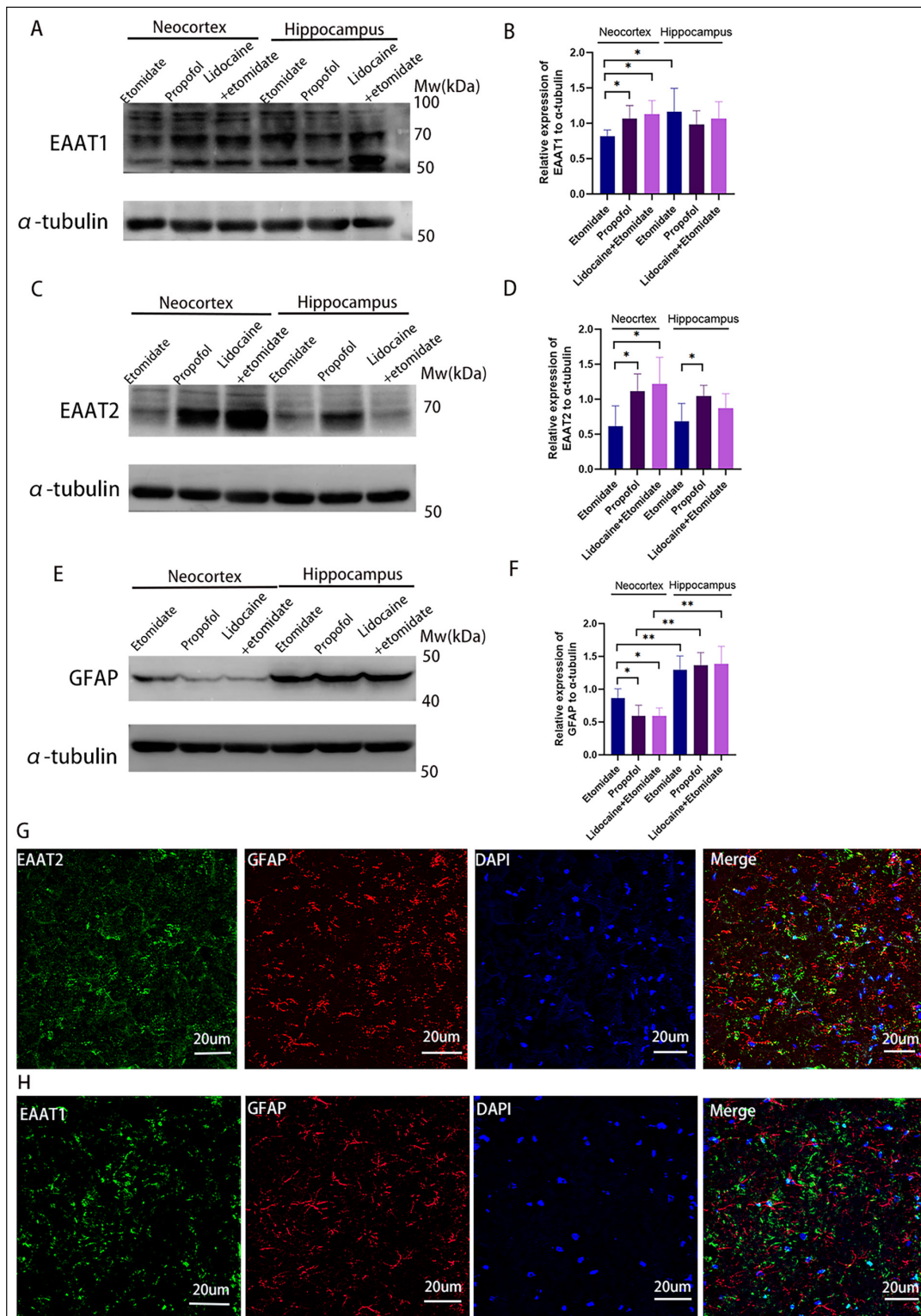


Figure 3. Localization of EAAT1 and EAAT2, and the proteins expression in neocortex and hippocampus. EAAT1 protein expression (A and B), EAAT2 protein expression (C and D) and GFAP protein expression (E and F) in the neocortex and hippocampus in the etomidate, propofol, and lidocaine plus etomidate group, one-way multiple comparisons ANOVA and paired *t* test were applied to analyze difference. Double immunofluorescence staining of GFAP (red) with EAAT1 (green) or EAAT2 (green) in neocortex. EAAT1 (H) and EAAT2 (G) were mainly expressed on astrocytes (n=4 rats, 5 pictures for each rat, scale bar=20 μ m). *: $p < 0.05$; **: $p < 0.01$.

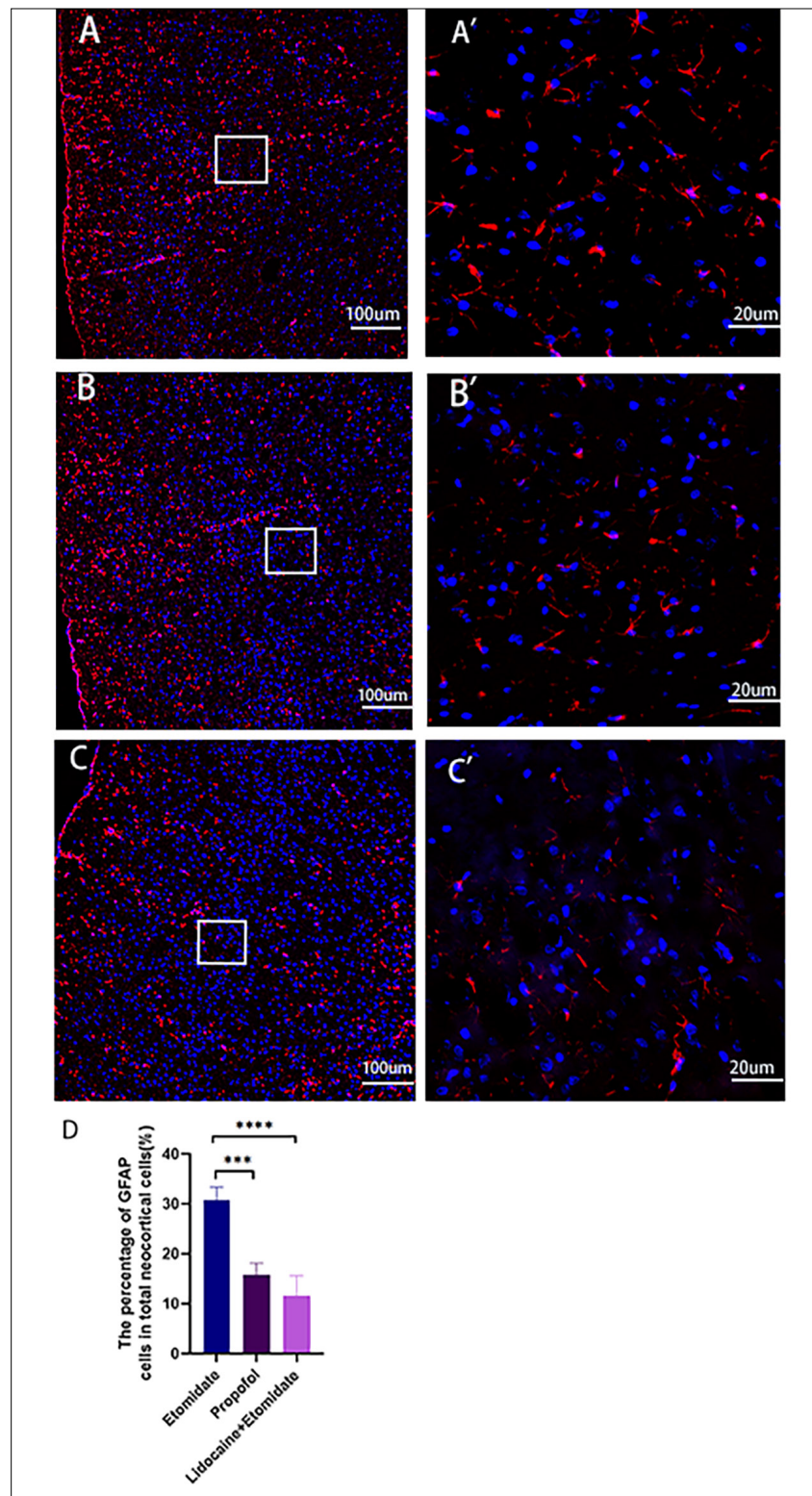


Figure 4. Effect of etomidate, propofol, lidocaine plus etomidate on the astrocyte response in neocortex. Etomidate group (A), Propofol group (B); Lidocaine plus etomidate group (C); Magnified images of A-C (A'-C'). Morphologically, astrocytes were observed under a 40×objective (Scale bars are 20 µm). The ratio of the number of astrocytes (labeled by GFAP) to the number of total cells (labeled by DAPI) was analyzed (D), as determined by one-way multiple comparisons ANOVA. Scale bars=100 µm (A-C), Scale bars=20 µm (A'-C'). ***: $p < 0.001$; ****: $p < 0.0001$.

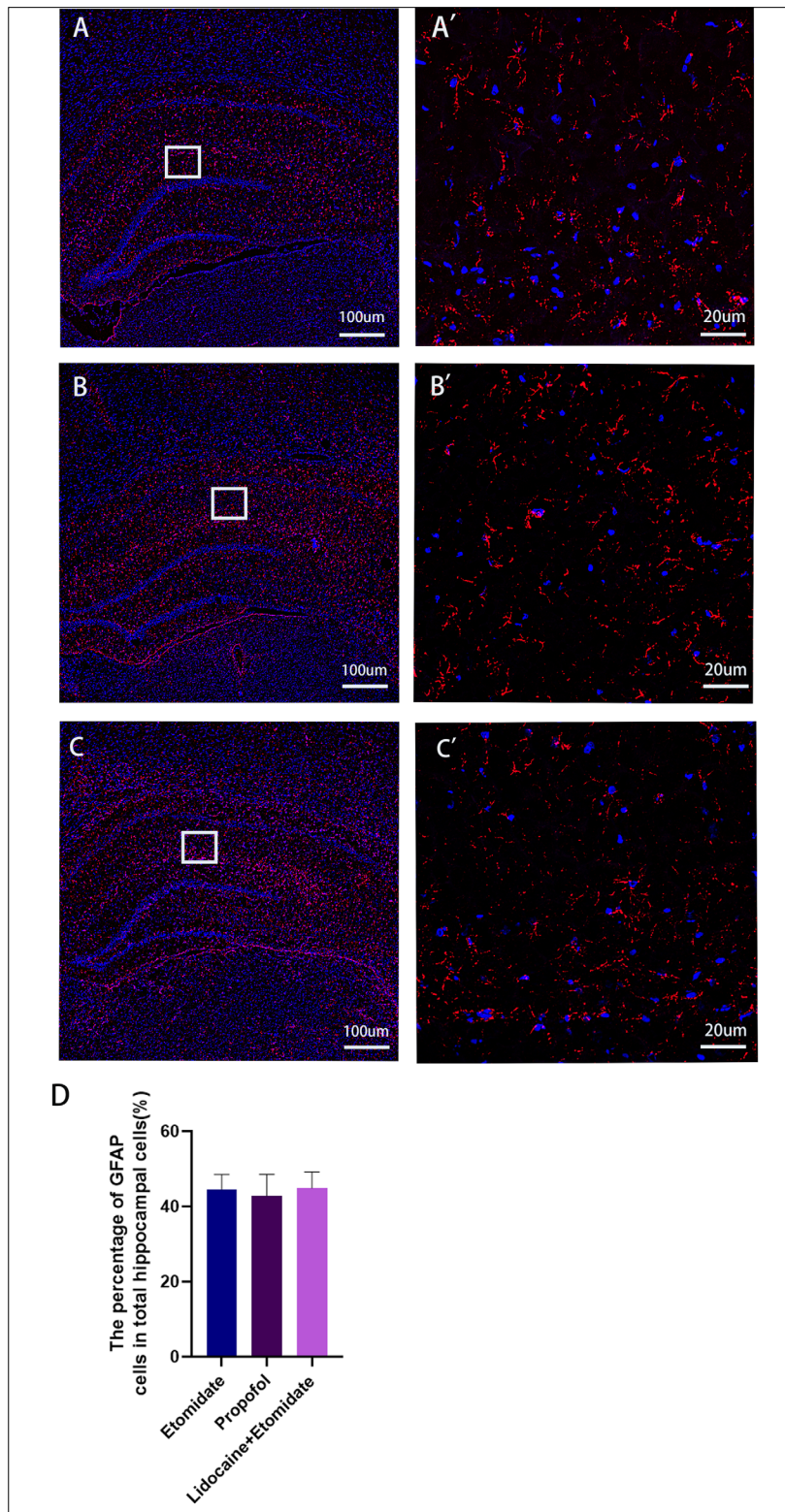


Figure 5. Effect of etomidate, propofol, lidocaine plus etomidate on the astrocyte response in hippocampus. Etomidate group (A), Propofol group (B); Lidocaine plus etomidate group (C); Magnified images of A-C (A'-C'). Morphologically, astrocytes were observed under a 40×objective (Scale bars are 20 µm). The ratio of the number of astrocytes (labeled by GFAP) to the number of total cells (labeled by DAPI) was analyzed (D), as determined by one-way multiple comparisons ANOVA. Scale bars=100 µm (A-C), Scale bars=20 µm (A'-C').

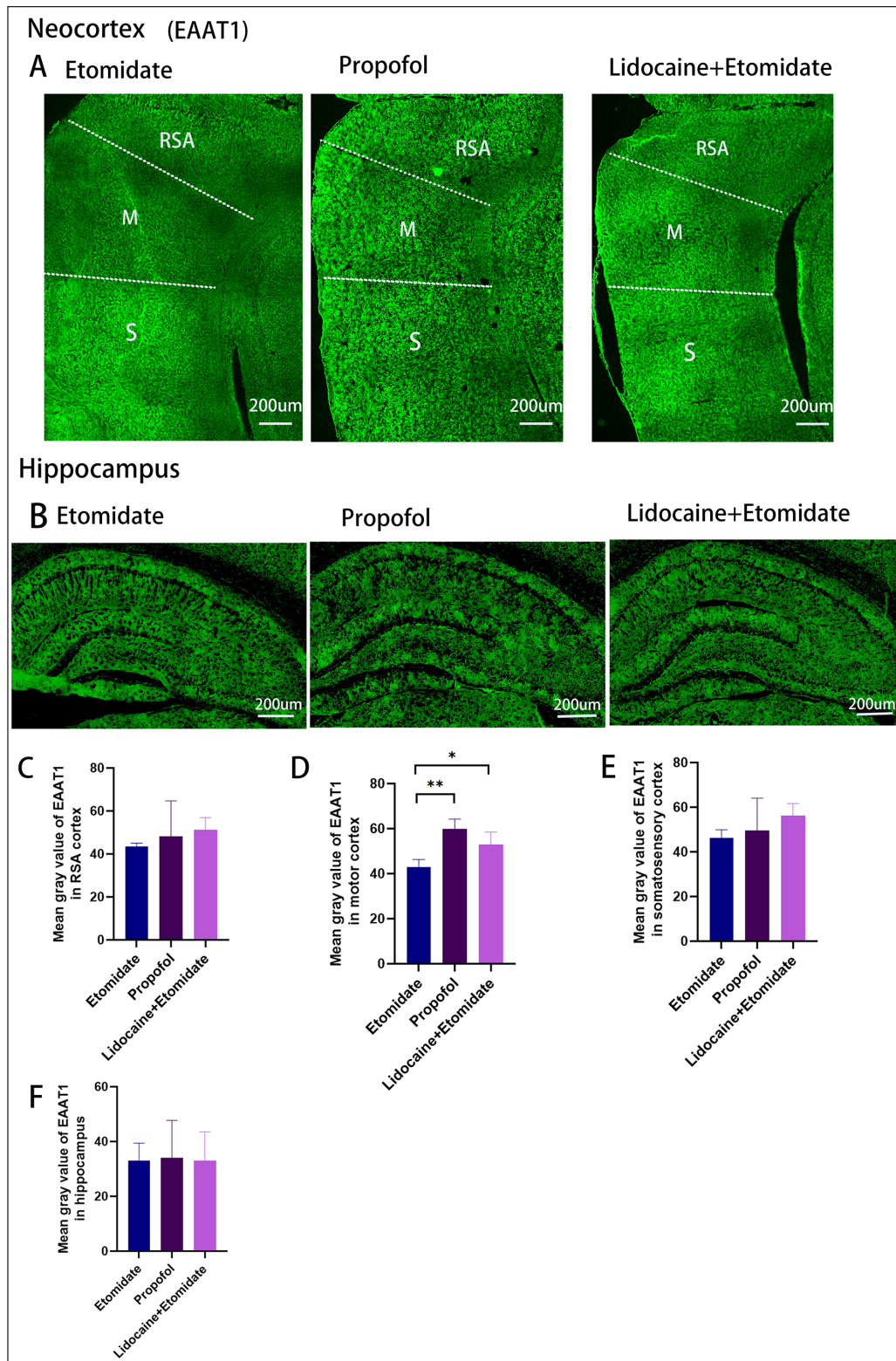


Figure 6. Immunofluorescence studies show that etomidate inhibited the expression of EAAT1 protein in motor cortex compared to the propofol and lidocaine plus etomidate group. Images of representative coronal sections stained for EAAT1 at 10 × magnification in neocortex (A) and hippocampus (B) in three groups. Quantification of EAAT1 immunoreactivity in RSA cortex (C), motor cortex (D), somatosensory cortex (E) and hippocampus (F). One-way multiple comparisons ANOVA was applied to analyze difference. Scale bars=200 µm. *: $p < 0.05$; **: $p < 0.01$. RSA: Retro splenial agranular.

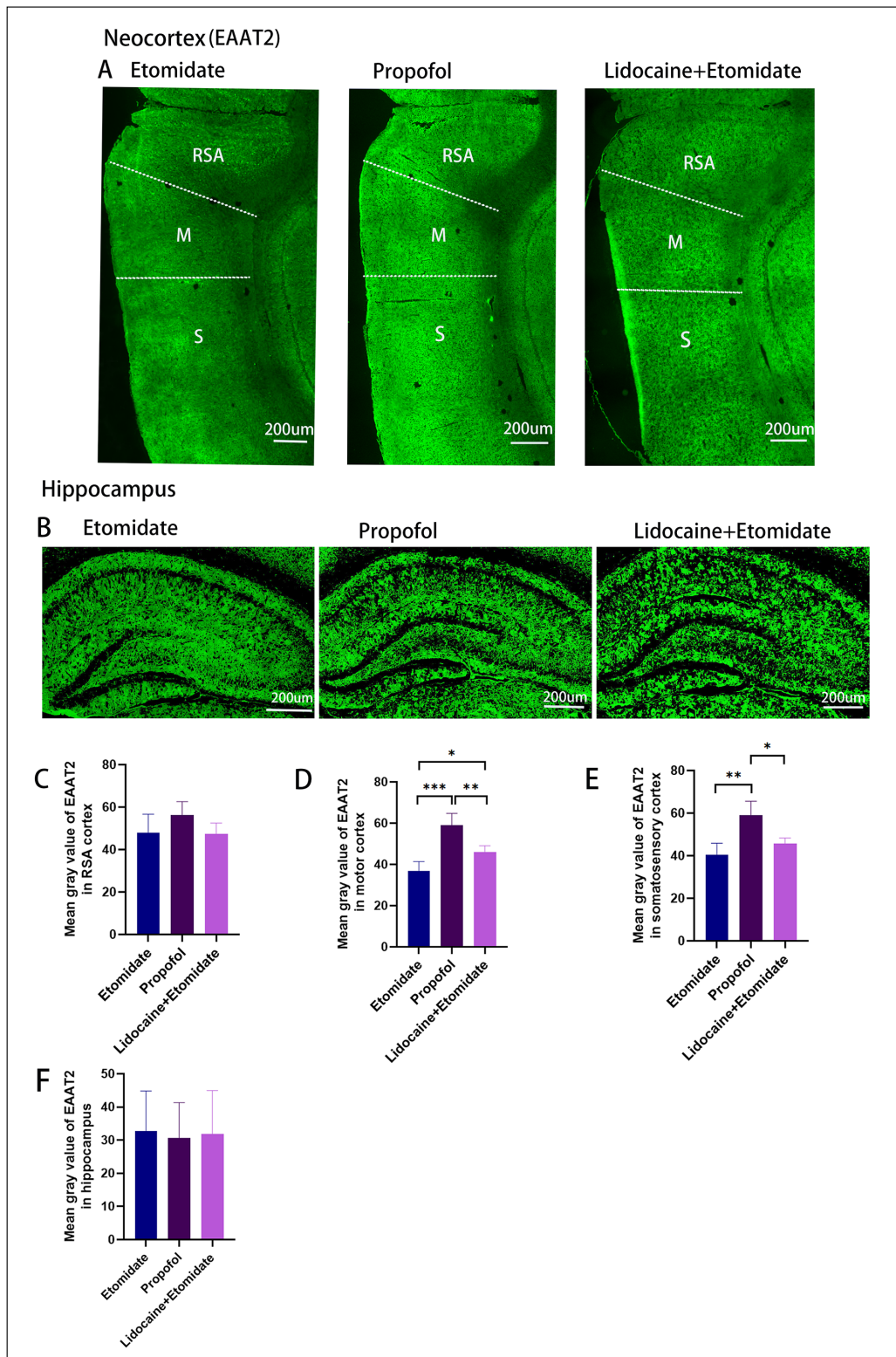


Figure 7. Immunofluorescence studies show that etomidate inhibited the expression of EAAT2 protein in motor cortex compared to the propofol and lidocaine plus etomidate group. Images of representative coronal sections stained for EAAT2 at 10 × magnification in neocortex (A) and hippocampus (B) in three groups. Quantification of EAAT1 immunoreactivity in RSA cortex (C), motor cortex (D), somatosensory cortex (E) and hippocampus (F). One-way multiple comparisons ANOVA was applied to analyze difference. Scale bars=200 µm. *: $p < 0.05$; **: $p < 0.01$; ***: $p < 0.001$. RSA: Retro splenial agranular.

not affect but propofol (59.16 ± 6.47 vs. 40.54 ± 5.39 , $n=4$, $p=0.0015$) increased the mean grey value of EAAT2 in the somatosensory cortex compared to the etomidate group, as determined by one-way multiple comparisons ANOVA.

Discussion

To investigate the effect of etomidate on excitatory neurotransmitter glutamate and the relationship between glutamate content in neocortex or hippocampus and myoclonus, we recorded the mean behavioral scores in three groups during anesthesia and conducted the glutamate levels in the CSF, neocortex and hippocampus. We found that etomidate increased mean behavioral scores and glutamate levels in the CSF and neocortex during anesthesia. More importantly, we demonstrated a strong correlation between the myoclonus and neocortical glutamate accumulation. The increased extracellular glutamate levels result in the imbalance of neurotransmitters and contribute to excessive excitability²⁵, such as seizures. EAAT1 and EAAT2, known to be distributed in astrocytes and responsible for glutamate uptake, play vital roles in balancing neurotransmitters²⁶. Moreover, GFAP, a member of the intermediate filament structural protein family that is predominantly expressed by astrocytes. To explore the effect of etomidate on the expression of EAATs and GFAP following myoclonus, we conducted the qPCR, western blot and immunofluorescence analysis. The results showed that etomidate did not affect EAAT1, EAAT2, or GFAP mRNA expression in the neocortex or hippocampus, but decreased the expression of EAAT1 and EAAT2 proteins, conversely activated the expression of GFAP protein in the neocortex, when compared with the propofol and lidocaine plus etomidate group. Together, the inconsistency in EAAT1, EAAT2, and GFAP gene and protein expression might be attributed to the differential location and timing of gene and protein expression under the action of the three anesthetic drugs²⁷. Translocation of membrane protein of EAAT1 in cell-surface can be regulated within minutes and faster; according to previous research²⁸, that can be possible by protein synthesis. Michaluk et al²⁹ also reported that EAAT2 dwells on the surface of rat brain astroglia, recycling with a lifetime of less than 1 min. Additionally, the rapid synthesis of GFAP intermediate filaments is typical characteristic for astrogliosis, which is well estab-

lished in the genesis of epilepsy³⁰. The decline in EAATs protein observed in the neocortex agrees with a previous study⁸ in which we showed that etomidate inhibited EAATs in cultures of cortical glial cells involving protein kinase A (PKA). In contrast, propofol increased the expression of EAAT2 in a brain injury model and protected hippocampal neurons³¹. Although the effect of lidocaine on EAATs have not been reported at present, systemic administration of lidocaine can effectively treat glutamate excitotoxicity-related brains³², which indicates that etomidate inhibits EAATs and the uptake of glutamate into astroglia probably *via* the modulation of protein phosphorylation. Recent studies³³ have suggested that the activity of glutamate transporters is regulated by the phosphorylation processes of PKA, protein kinase C (PKC) and phosphatidylinositol-3-kinase (PI3K), and these regulatory effects could be associated with a rapid change in the number of transporters within the plasma membrane.

The induction of GFAP-positive cells by etomidate in the neocortex in a short period may reflect a process in which seizures induce astrocytic hypertrophy and may also be related to brain damage³⁴ with stress response. The decline in GFAP expression observed in propofol and lidocaine plus etomidate in the neocortex agrees with a previous study in which we showed that pretreatment with propofol decreased the number of GFAP-positive cells in rat cerebrocortical slices³⁵ and that lidocaine had a neuroprotective effect and reduced astrocytic activation and inflammation by downregulating GFAP³⁶. Immediate astrocyte degeneration and the downregulation of their expression in astrocytes³⁷ and compensatory astrogliosis may explain the opposite changes of EAATs and GFAP after etomidate. In addition, in contrast with the RSA, somatosensory cortex and hippocampus, the motor cortex seemed to be the region where the expression levels of EAATs were declined after intravenous administration of etomidate, compared to the propofol or lidocaine plus etomidate. Since the sensitivity of the different regions to etomidate also differs due to the difference in the distribution of γ -aminobutyric acid (GABA) receptor subtypes and reactive astrogliosis, it may be part of the early-term response triggered by etomidate treatment in different brain regions^{38,39}.

Limitations

There are some limitations of our experiment. First, only male rats were chosen in our study, since the estrogen levels of male animals are

more stable than those of female animals. To exclude the influence of estrogen level fluctuation⁴⁰, only male rats were included. Second, we did not conduct an experiment on the effects on etomidate-induced myoclonus by regulating the phosphorylation of EAATs. Adolph et al⁴¹ provided evidence that blockage of the PKA pathway rapidly upregulated glutamate uptake by mediating EAAT1. We will conduct relevant experiments to verify the effect of the PKA pathway on the etomidate triggering phosphorylation of EAATs and explore a new rapid therapeutic target for etomidate-induced myoclonus.

Conclusions

Etomidate-induced myoclonus is associated with neocortical glutamate accumulation. Suppression of the astrogliosis in neocortex and promoting extracellular glutamate uptake by regulating glutamate transporters (EAATs) in the motor cortex may be the therapeutic target for prevention of etomidate-induced myoclonus.

Conflict of Interest

The Authors declare that they have no conflict of interests.

Acknowledgements

Not applicable.

Ethics Approval

The protocol in this experiment was approved by the Animal Ethics Committee of West China Hospital, Sichuan University (ethical approval No.: 20211423A) and conducted in strict accordance with the Guide for the Care and Use of Laboratory Animals.

Funding

None.

Availability of Data and Materials

The datasets used and/or analyzed during the current study are available from the corresponding author upon reasonable request.

References

- 1) He L, Ding Y, Chen H, Qian Y, Li Z. Butorphanol pre-treatment prevents myoclonus induced by etomidate: a randomised, double-blind, controlled clinical trial. *Swiss Med Wkly* 2014; 144: w14042.
- 2) Kojovic M, Cordivari C, Bhatia K. Myoclonic disorders: a practical approach for diagnosis and treatment. *Ther Adv Neurol Disord* 2011; 4: 47-62.
- 3) Hua J, Miao S, Shi M, Tu Q, Wang X, Liu S, Wang G, Gan J. Effect of butorphanol on etomidate-induced myoclonus: a systematic review and meta-analysis. *Drug Des Devel Ther* 2019; 13: 1213-1220.
- 4) Hao L, Hu X, Zhu B, Li W, Huang X, Kang F. Clinical observation of the combined use of propofol and etomidate in painless gastroscopy. *Medicine (Baltimore)* 2020; 99: e23061.
- 5) Liu J, Liu R, Meng C, Cai Z, Dai X, Deng C, Zhang J, Zhou H. Propofol decreases etomidate-related myoclonus in gastroscopy. *Medicine* 2017; 96: e7212.
- 6) Lang B, Zhang L, Yang C, Lin Y, Zhang W, Li F. Pretreatment with lidocaine reduces both incidence and severity of etomidate-induced myoclonus: a meta-analysis of randomized controlled trials. *Drug Des Devel Ther* 2018; 12: 3311-3319.
- 7) Voss LJ, Sleigh JW, Barnard JP, Kirsch HE. The howling cortex: seizures and general anesthetic drugs. *Anesth Analg* 2008; 107:1689-1703.
- 8) R  th M, F  hr K.J, Weigt HU, Gauss A, Engele J, Georgieff M, K  ster S, Adolph O. Etomidate reduces glutamate uptake in rat cultured glial cells: involvement of PKA. *Br J Pharmacol* 2008; 155: 925-933.
- 9) Green JL, Dos Santos WF, Fontana ACK. Role of glutamate excitotoxicity and glutamate transporter EAAT2 in epilepsy: Opportunities for novel therapeutics development. *Biochem Pharmacol* 2021; 193: 114786.
- 10) Schneider N, Cordeiro S, Machtens JP, Braams S, Rauen T, Fahlke C. Functional properties of the retinal glutamate transporters GLT-1c and EAAT5. *J Biol Chem* 2021; 289: 1815-1824.
- 11) Pajarillo E, Digman A, Nyarko-Danquah I, Son DS, Soliman KFA, Aschner M, Lee E. Astrocytic transcription factor REST upregulates glutamate transporter GLT1, protecting dopaminergic neurons from manganese-induced excitotoxicity. *J Biol Chem* 2021; 297: 101372.
- 12) Murphy-Royal C, Dupuis JP, Varela JA, Panatier A, Pinson B, Baufreton J, Groc L, Oliet SH. Surface diffusion of astrocytic glutamate transporters shapes synaptic transmission. *Nat Neurosci* 2015; 18: 219-226.
- 13) Hubbard JA, Hsu MS, Fiocco TA, Binder DK. Glial cell changes in epilepsy: overview of the clinical problem and therapeutic opportunities. *Neurochem Int* 2013; 63: 638-651.
- 14) Mukherjee S, Arisi GM, Mims K, Hollingsworth G, O'Neil K, Shapiro LA. Neuroinflammatory mechanisms of post-traumatic epilepsy. *J Neuroinflammation* 2020; 17: 193.
- 15) Sofroniew MV. Multiple roles for astrocytes as effectors of cytokines and inflammatory mediators. *Neuroscientist* 2014; 20: 160-172.

- 16) Xu S, Sun Q, Fan J, Jiang Y, Yang W, Cui Y, Yu Z, Jiang H, Li B. Role of astrocytes in post-traumatic epilepsy. *Front Neurol* 2019; 10: 1149.
- 17) Voss LJ, Andersson L, Jadelind A. The general anesthetic propofol induces ictal-like seizure activity in hippocampal mouse brain slices. *Springerplus* 2015; 4: 816.
- 18) National Research Council Committee for the Update of the Guide for the Care and Use of Laboratory Animals. *The National Academies Collection: Reports Funded by National Institutes of Health. Guide for the Care and Use of Laboratory Animals*. Washington (DC): National Academies Press (US), 2011.
- 19) Kim YS, Kim SH, Shin J, Harikishore A, Lim JK, Jung Y, Lyu HN, Baek NI, Choi KY, Yoon HS, Kim KT. Luteolin suppresses cancer cell proliferation by targeting vaccinia-related kinase 1. *PLoS One* 2014; 9: e109655.
- 20) Yuan X, Fu Z, Ji P, Guo L, Kassab RB, Alkandiri A, Habotta OA, Abdel Moneim AE, Kassab RB. Selenium nanoparticles pre-treatment reverse behavioral, oxidative damage, neuronal loss and neurochemical alterations in pentylenetetrazole-induced epileptic seizures in mice. *Int J Nanomedicine* 2020; 15: 6339-6353.
- 21) Sun JY, Zhao SJ, Wang HB, Hou YJ, Mi QJ, Yang MF, Yuan H, Ni QB, Sun BL, Zhang ZY. Ifenprodil Improves Long-Term Neurologic Deficits Through Antagonizing Glutamate-Induced Excitotoxicity After Experimental Subarachnoid Hemorrhage. *Transl Stroke Res* 2021; 12: 1067-1080.
- 22) Santos PS, Campêlo LM, Freitas RL, Feitosa CM, Saldanha GB, Freitas RM. Lipoic acid effects on glutamate and taurine concentrations in rat hippocampus after pilocarpine-induced seizures. *Arq Neuropsiquiatr* 2011; 69: 360-364.
- 23) Hanson E, Armbruster M, Cantu D, Andresen L, Taylor A, Danbolt NC, Dulla CG. Astrocytic glutamate uptake is slow and does not limit neuronal NMDA receptor activation in the neonatal neocortex. *Glia* 2015; 63: 1784-1796.
- 24) Liu Y, Ding XF, Wang XX, Zou XJ, Li XJ, Liu YY, Li J, Qian XY, Chen JX. Xiaoyaosan exerts antidepressant-like effects by regulating the functions of astrocytes and EAATs in the prefrontal cortex of mice. *BMC Complement Altern Med* 2019; 19: 215.
- 25) Rakhade SN, Loeb JA. Focal reduction of neuronal glutamate transporters in human neocortical epilepsy. *Epilepsia* 2008; 49: 226-236.
- 26) Kim K, Lee SG, Kegelman TP, Su ZZ, Das SK, Dash R, Dasgupta S, Barral PM, Hedvat M, Diaz P, Reed JC, Stebbins JL, Pellicchia M, Sarkar D, Fisher PB. Role of excitatory amino acid transporter-2 (EAAT2) and glutamate in neurodegeneration: opportunities for developing novel therapeutics. *J Cell Physiol* 2011; 226: 2484-2493.
- 27) Odeon MM, Andreu M, Yamauchi L, Grosman M, Acosta GB. Chronic postnatal stress induces voluntary alcohol intake and modifies glutamate transporters in adolescent rats. *Stress* 2015; 18: 427-434.
- 28) NC Danbolt. Glutamate uptake. *Prog Neurobiol* 2001; 65: 1-105.
- 29) Michaluk P, Heller JP, Rusakov DA. Rapid recycling of glutamate transporters on the astroglial surface. *Elife* 2021; 10: e64714.
- 30) Lee DJ, Hsu MS, Seldin MM, Arellano JL, Binder DK. Decreased expression of the glial water channel aquaporin-4 in the intrahippocampal kainic acid model of epileptogenesis. *Exp Neurol* 2012; 235: 246-255.
- 31) Gong HY, Zheng F, Zhang C, Chen XY, Liu JJ, Yue XQ. Propofol protects hippocampal neurons from apoptosis in ischemic brain injury by increasing GLT-1 expression and inhibiting the activation of NMDAR via the JNK/Akt signaling pathway. *Int J Mol Med* 2016; 38: 943-950.
- 32) Chiu KM, Lu CW, Lee MY, Wang MJ, Lin TY, Wang SJ. Neuroprotective and anti-inflammatory effects of lidocaine in kainic acid-injected rats. *Neuroreport* 2016; 27: 501-507.
- 33) Guillet BA, Velly LJ, Canolle B, Masméjean FM, Nieoullon AL, Pisano P. Differential regulation by protein kinases of activity and cell surface expression of glutamate transporters in neuron-enriched cultures. *Neurochem Int* 2005; 46: 337-346.
- 34) Chen N, Liu C, Yan N, Hu W, Zhang JG, Ge Y, Meng FG. A macaque model of mesial temporal lobe epilepsy induced by unilateral intrahippocampal injection of kainic acid. *PLoS One* 2013; 8: e72336.
- 35) Zhou XF, Huang DD, Wang DF, Fu JQ. The protective effect of propofol pretreatment on glutamate injury of neonatal rat brain slices. *Zhongguo Wei Zhong Bing Ji Jiu Yi Xue* 2012; 24: 750-753.
- 36) Chou TH, Musada GR, Romano GL, Bolton E, Porciatti V. Anesthetic Preconditioning as Endogenous Neuroprotection in Glaucoma. *Int J Mol Sci* 2018; 19: 237.
- 37) Sheldon AL, Robinson MB. The role of glutamate transporters in neurodegenerative diseases and potential opportunities for intervention. *Neurochem Int* 2007; 51: 333-355.
- 38) Rojas-Castañeda JC, Viguera-Villaseñor RM, Chávez-Saldaña M, Rojas P, Gutiérrez-Pérez O, Rojas C, Arteaga-Silva M. Neonatal exposure to monosodium glutamate induces morphological alterations in suprachiasmatic nucleus of adult rat. *Int J Exp Pathol* 2016; 97: 18-26.
- 39) Sieghart W. Structure and pharmacology of gamma-aminobutyric acid A receptor subtypes. *Pharmacol Rev* 1995; 47: 181-234.
- 40) Allais G, Chiarle G, Sinigaglia S, Airola G, Schiapparelli P, Benedetto C. Estrogen, migraine, and vascular risk. *Neurol Sci* 2018; 39: 11-20.
- 41) Adolph O, Köster S, Rähm M, Georgieff M, Weigt HU, Engele J, Senftleben U, Föhr KJ. Rapid increase of glial glutamate uptake via blockade of the protein kinase A pathway. *Glia* 2007; 55: 1699-1707.